

MULTIMODAL IMAGING IN THE CONGENITAL PULMONARY LYMPHANGIECTASIA-CONGENITAL CHYLOTHORAX-HYDROPS FETALIS CONTINUUM

C. Bellini, M. Mazzella, C. Campisi, G. Taddei, F. Mosca, P. Tomà, G. Villa,
F. Boccardo, A.R. Sementa, R.C. Hennekam, G. Serra

Servizio di Patologia Neonatale (CB,MM,GS), Dipartimento di Pediatria, Università di Genova, Istituto G. Gaslini, Genova; Dipartimento di Scienze Chirurgiche Specialistiche Anestesiologiche e Trapianti d'Organi (CC,FB), Università di Genova, Genova; Dipartimento di Medicina Interna (GT), Università di Genova, Genova; A.O. Istituti Clinici di Perfezionamento (FM), U.O. Neonatologia, Milano; Servizio di Radiologia (PT), Istituto G. Gaslini, Genova; Servizio di Anatomia Patologica (ARS), Istituto G. Gaslini, Genova, Italia; Department of Pediatrics/Clinical Genetics (RCH), Academic Medical Center, University of Amsterdam, The Netherlands

ABSTRACT

We report on three infants with congenital chylothorax (CC) and congenital pulmonary lymphangiectasia (CPL). CPL appears to be a characteristic pathological finding in CC. Through the use of lymphoscintigraphy and computed tomography, this study suggests that CC and CPL are strongly correlated entities and that the dysplasia of the lymphatic system results in a pulmonary lymphatic obstruction sequence. The initial microscopic dilatation of the lymph channels may lead to progressive weeping of lymphatics and, consequently, to pleural effusion. Non-Immune Hydrops Fetalis (NIHF) may be the final consequence of impaired systemic venous return and may help to explain pleural-pulmonary involvement in this generalized lymph-vessel malformation syndrome.

Congenital pulmonary lymphangiectasia (CPL) is a rare congenital anomaly that was first described by Virchow in 1896 (1). CPL is characterized by numerous dilated lymphatic channels in the pleura, interlobular septa, and bronchovascular axes. Chylothorax is defined as an accumulation of chyle in the pleural

space. The term congenital chylothorax (CC) is usually limited to congenital abnormalities of the lymphatic system presenting at birth (2). Chylothorax itself is a common end-point for a variety of pathological processes including intrinsic abnormalities of the lymphatic system and disruption of the thoracic duct due to trauma, surgery, malignancy, or cardiovascular disease. Non-Immune Hydrops Fetalis (NIHF) is a rare consequence of fetal pleural effusion (3). No anatomic descriptions of CPL-CC-NIHF in neonates have been reported (4), and only sparse data are available regarding children (5). The same pathogenetic mechanisms that lead to pleural effusion may also produce NIHF but no conclusive documentation has been reported. This paper focuses on the CPL-CC-NIHF continuum in neonates, and on the basis of radiological and lymphoscintigraphic evaluation, it is suggested that there is a strong correlation among these entities.

CLINICAL REPORTS

Case 1

The patient, a female, the second child of

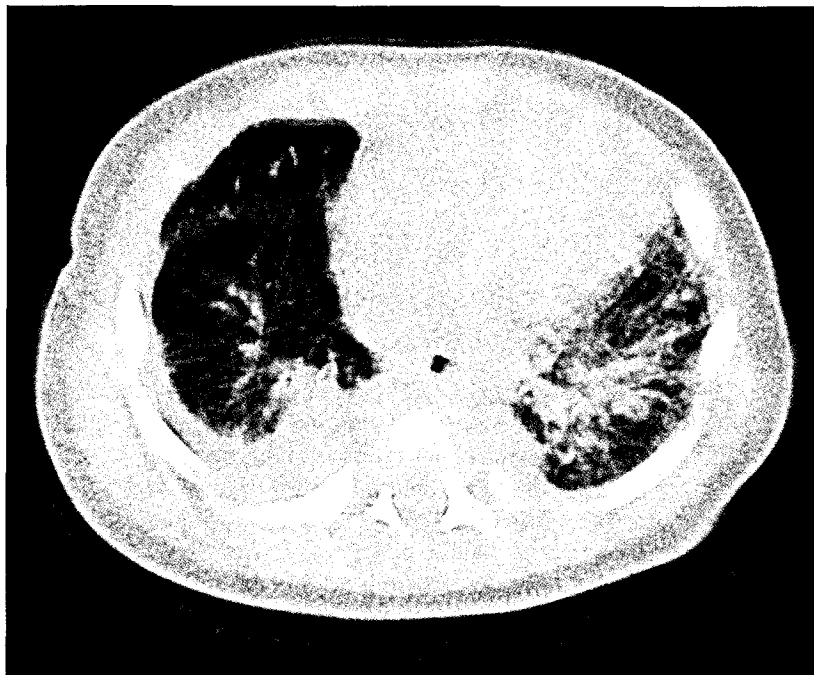


Fig. 1. Case 1. High-resolution computed tomography shows diffuse thickening of the interstitium, both peribronchovascular and within the septa surrounding the lobules.

healthy, unrelated parents, was born prematurely at 33 weeks of age by vaginal delivery. During pregnancy, polyhydramnios was evident at 30 weeks of gestation. At birth, her weight was 2,900 g, length was 47 cm, and occipito-frontal circumference was 33 cm, all parameters between the 75th and 90th percentiles. Immediate intubation and artificial ventilation were performed to treat severe respiratory distress. Bilateral pleural effusions required surgical drainage for the first 8 days of life. The pleural fluid showed a glucose content of 75 mg/dl (total protein content of 1.63 g/dl) and a triglyceride content of 970 mg/dl. Chylothorax was diagnosed on day 5 on the basis of the criteria of van Straaten et al (3) and Straats et al (6).

The patient was initially fed solely by means of parenteral nutrition. Starting on the third day, she was enterally fed on standard formula alone. On the 10th day, a medium-chain triglyceride formula (Portagen R) was added for approximately 10 days. The patient

was then switched to standard formula as the pleural effusions significantly decreased.

Phenotypic features included hypertelorism, a flat face, with a broad, depressed nasal bridge, a bulbous nasal tip, small mouth, and low-set ears. The skin appeared marbled. Fetal pads were evident. Generalized lymphedema was present, especially prominent in the lower right arm and hand, the lower right leg and foot, and the genitalia.

Laboratory examination showed severe hypoproteinemia on repeated evaluations (serum total protein levels averaged ~3.5 g/dl with albumin levels ~2 g/dl) and hypogammaglobulinemia (IgG 237 mg/dl, IgA 28 mg/dl, IgM 8 mg/dl). The leukocyte count was in the low normal range (4,000-6,000/mm³). Serum electrolyte levels remained within normal limits. Renal function was normal, and there was no proteinuria. Repeated examinations of fecal excretion of alpha-1-antitrypsin showed elevated values (550-650/g wet feces [normal 7.7-159/g wet feces]), suggesting

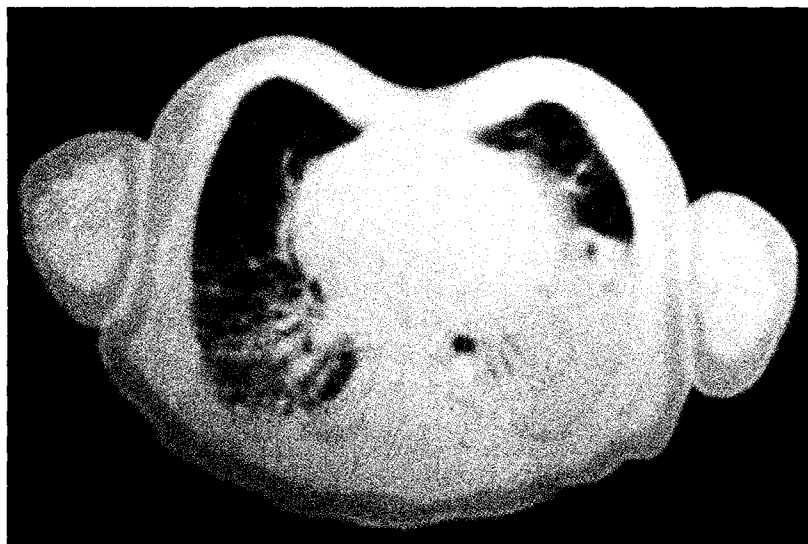


Fig. 2. Case 2, 55 days. Helical chest CT (slice thickness 3.0 mm, pitch 1.5, reconstruction interval 3.0 mm) shows diffuse interstitial changes with thickening of the interlobular septa in the right chest (left side of image) associated with contralateral pleural fluid collection and atelectasis.

intestinal lymphangiectasia with protein losing enteropathy. The parents refused a duodenal biopsy. Chromosome studies showed a normal female karyotype (46, XX, high-resolution, 750 band level). Other investigations (TORCHES-CLAP titer; plasma 7-dehydrocholesterol level; renal and cardiac ultrasonography) yielded normal results. The initial chest X-ray showed totally opaque enlarged lung fields. After drainage of the pleural fluid, pleural opacity progressively decreased.

In the first months of life, the X-ray pattern was characterized by increased interstitial markings. High-Resolution Computed Tomography (HRCT) was performed when the patient was 45 days old (*Fig. 1*) using 2.0 mm thick sections at 10-mm intervals. HRCT on the left side showed diffuse thickening of the interstitium, peribronchovascular interstitium, and septa surrounding the lobules. On the right side, pleural effusion and thickening of the interlobar fissures were observed.

At the age of 55 days, radionuclide lymphoscintigraphy (Lymphoscint,

Amersham Health) showed abnormal drainage of the right lower limb and thoracic duct. Initial dermal backflow was evident in the distal portion of the right hand and foot, reflecting accumulation of the radiocolloid in dilated dermal lymphatic channels. Tracer accumulation within the thoracic duct was also evident (*Fig. 4a,b*). The patient is well one year later.

Case 2

The patient was the first-born child of healthy, unrelated parents. She was born prematurely at 33 weeks of age. At birth her weight was 2,300 g, length was 46.5 cm, and occipito-frontal circumference was 32.5 cm; all parameters were between the 75th and 90th percentiles. She was intubated at birth and placed on a ventilator for 5 days, initially at high pressure levels, and then treated by nasal continuous positive airway pressure (nCPAP). Bilateral trans-thoracic drains were immediately inserted because of bilateral pleural effusions. Surgical drainage was needed for 40 days. After feeding with



Fig. 3. Case 2. Coronal MRI T1-WSE displays thickening of the interstitium on the right (left side of image) and pleural fluid collection and atelectasis on the left.

standard formula was started, chylothorax was diagnosed on day 7 based on the criteria of van Straaten et al (3) and Straats et al (6).

Phenotypic features included coarse face, high forehead, full and hanging cheeks, low-set and dysplastic ears, and highly expressed persistent fetal finger-pads. There was neither peripheral nor generalized lymphedema.

Laboratory examinations showed mild hypoproteinemia on repeated evaluations (total serum protein levels averaged ~5.5 g/dl; albumin levels ~3.8 g/dl) and hypogammaglobulinemia (IgG 96 mg/dl, IgA 6 mg/dl, IgM 36 mg/dl). The leukocyte count and serum electrolyte levels were within the normal range. Renal function was normal, and there was no proteinuria. Repeated examinations of fecal excretion of alpha-1-antitrypsin showed elevated values (~450/g wet feces), suggesting intestinal lymphangiectasia and protein-losing

enteropathy. Chromosome studies showed a normal female karyotype (46, XX, high-resolution, 750 band level). Other investigations (TORCHES-CLAP titer; renal ultrasonography) yielded normal results. Ultrasound (US) examinations of the heart showed neither anatomic abnormalities nor pericardial effusion. Thoracic radiographs showed increased interstitial markings. Diffuse thickening of the peribronchovascular interstitium and the septa surrounding the lobules was confirmed at 55 days of age by High-Resolution Computed Tomography (Fig. 2). Coronal MRI T1-WSE displayed thickening of the interstitium on the right and pleural fluid collection and atelectasis on the left (Fig. 3). Axial MRI T2-WSE showed high-signal material within the right pulmonary interstitium, associated with pleural effusion on the left (*data not shown*). At the age of 95 days, radionuclide

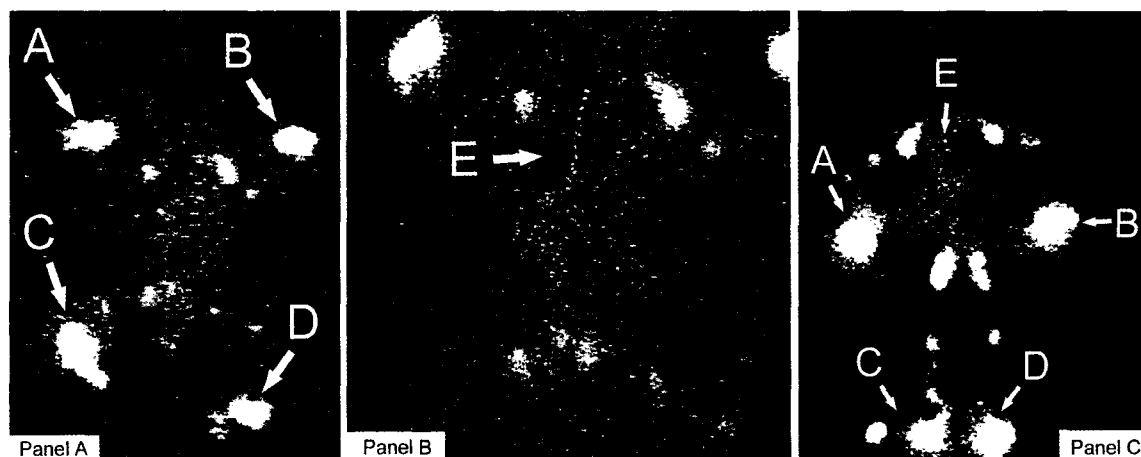


Fig. 4. Panels A and B: case 1. Panel C: case 2. Arrows A, B, C, and D indicate the right hand, left hand, right foot, and left foot, respectively. Arrow E indicates the thoracic duct. Lymphangioscintigraphic images were obtained following intradermal injection of Tc-99m microcolloidal sulfide (Lymphoscint, Nanocool, Solco Basel, Ltd, Basel Switzerland). Images were obtained approximately 5 minutes after completion of the simultaneous injections in the 4 limbs. Case 1. Panels A and B. Tracer accumulation is evident in the distal portion of both lower limbs, along with tracer accumulation (presence) within the thoracic duct (arrow E), indicating radiocolloid transport in the superficial dermal lymphatics and persistence in the thoracic duct. Case 2. Panel C. Rapid transport of the tracer was evident in the right lower limb, consistent with lymphatic hyperplasia. Initial dermal backflow is seen in the distal portion of the hand and foot reflecting radiocolloid transport in the superficial channels of the dermis. Tracer accumulation in the thoracic duct is also seen (arrow E). Visual findings of lymphoscintigraphy are evaluated by determination of a numeric index of transport kinetics (16). Case 1. The transport index in both upper limbs and the lower left limb was normal (TI= 2), while the TI of the lower right limb was pathological (right limb: TI= 45). Case 2. The TI of four limbs was normal (TI= 2). TI was calculated from the formula: $TI = K + D + 0.04T + N + V$, where K is lymphatic transport kinetics (no delay, low grade delay, extreme delay, lack of transport are 0, 3, 5, and 9, respectively), D is the distribution pattern of the tracer (normal, partial diffuse, diffuse, transport stop are 0, 3, 5, and 9, respectively), T is the time in minutes of tracer appearance in the lymph nodes (no appearance is 9), V is the ratio between the visualization of lymph vessels and graft (nodes and vessels, respectively, clearly demonstrated, faint visualization, hardly recognizable, no visualization are 0, 3, 5, and 9, respectively). Each parameter ranges from 0 to 9, so total score ranges from 0 (normal) to 45 (pathological) (16).

lymphoscintigraphy (Lymphoscint, Amersham Health) was performed. Rapid drainage of the tracer was especially evident in the right lower limb, suggesting possible lymphatic hyperplasia. Initial dermal backflow was seen in the distal portion of the hand and foot, reflecting an accumulation of the radiocolloid in the dilated dermal lymphatic channels. The thoracic duct was prominently visualized (Fig. 4c). The patient is well one year later.

Case 3

The patient was the first-born child of healthy, unrelated parents. He was born

prematurely at 34 weeks of age. At birth his weight was 1,895 g, length was 43 cm, and occipito-frontal circumference was 31 cm, all parameters between the 25th and 50th percentiles. At birth, he needed immediate resuscitation (APGAR score at the 1st minute was 1), and he was intubated and mechanically ventilated for the next 38 days. Due to asymmetric pleural effusion, a unilateral right transthoracic drain was immediately inserted (it was removed after 30 days). Chylothorax was diagnosed after starting enteral feeding (day 12) on the basis of the criteria of van Straaten et al (3) and Straats et al (6). No generalized or peripheral

lymphedema was evident. The patient showed persistent hypotonia, possibly related to the severe asphyxia he had suffered at birth. Hypoproteinemia (total serum protein 3.9 g/dl, albumin 2.5 g/dl) and hypogammaglobulinemia (IgG 265 mg/dl, IgA 21 mg/dl, and IgM 28 mg/dl) were noted. Blood leukocyte count, serum electrolytes, and renal function were normal. Metabolic work-up, including plasma glucose, lactic and pyruvic acids, and ammonia were within the normal range as were plasma and urine aminoacids and VLFCA. US examination failed to demonstrate pericardial effusion or ascites, and no anatomical anomalies were found in the heart, kidney, liver, or spleen. Brain US revealed the presence of periventricular leukomalacia and dilated cerebral ventricles. Thoracic radiographs showed increased interstitial markings. High-Resolution Computed Tomography was performed at 46 days of age and confirmed diffuse thickening of both the peribronchovascular interstitium and the septa surrounding the lobules (not shown). The patient's unstable clinical condition ruled out lymphoscintigraphy. The patient died of septic shock on day 53 of life. Post-mortem evaluation of the lungs and pleura showed the presence of a pulmonary lobular pattern accentuated by a reticulum of white lines corresponding to thickened interlobular septa. On post-mortem histological examination, dilated lymph vessels were detected in the sub-pleural connective tissue, interlobular septa, and along bronchovascular bundles (*Fig. 5*). No anomalies were found in the brain, liver, intestine or skin.

DISCUSSION

Congenital pulmonary lymphangiectasia is a rare developmental disorder of the pulmonary lymphatics that is characterized by numerous dilated lymphatic channels in the sub-pleural connective tissue, interlobular septa, and along bronchovascular axes. CPL usually occurs sporadically, although

autosomal recessive inheritance has also been suggested (7,8). CPL has also been associated with multiple congenital anomaly syndromes such as Noonan syndrome, Turner syndrome, Down syndrome (7), Frijns syndrome (5), Hennekam syndrome (9), as well as with 46,XY/46,XX mosaicism and ichthyosis congenita (5). Noonan et al (10) divided CPL into 3 categories: a) component of generalized lymphangiectasia, b) secondary to cardiac defects producing obstruction to pulmonary venous blood flow, and c) primary pulmonary developmental defect.

Congenital chylothorax (CC) is the accumulation of chyle or intestinal lymph in the pleural cavity at birth and is the most frequent type of pleural effusion in the newborn (7). Early death is usually caused by associated severe pulmonary hypoplasia. The diagnosis of CC is generally confirmed in surviving newborns by thoracentesis.

The incidence is approximately 1:10,000-15,000 pregnancies, with a male-female ratio of 2:1 (11, 12). The right side of the thorax is usually affected, and bilateral chylothorax is quite rare (12). Perinatal mortality is high varying from 46% in cases with isolated pleural effusion to as high as 98% when it occurs together with NIHF, when gestational age is 32 weeks or less, or when no prenatal treatment is given (11,12).

Chyle (or intestinal lymph) contains a variety of components, including fats (mainly phospholipids, cholesterol, and triglycerides) and proteins (mainly albumin, immunoglobulins, and fibrinogen). Electrolytes and fat-soluble vitamins in concentrations similar to those found in plasma as well as significant numbers of lymphocytes are also detectable (13). Chylothorax is usually diagnosed in the presence of a pleural effusion with a triglyceride level >1.1 mmol/L and a cell count $>1,000$ cells/mm³ with a predominance of lymphocytes (~80%), according to the criteria of van Straaten et al (3) and by Straats et al (6). However, this is an unreliable diagnostic test in malnourished patients and in patients not receiving enteral

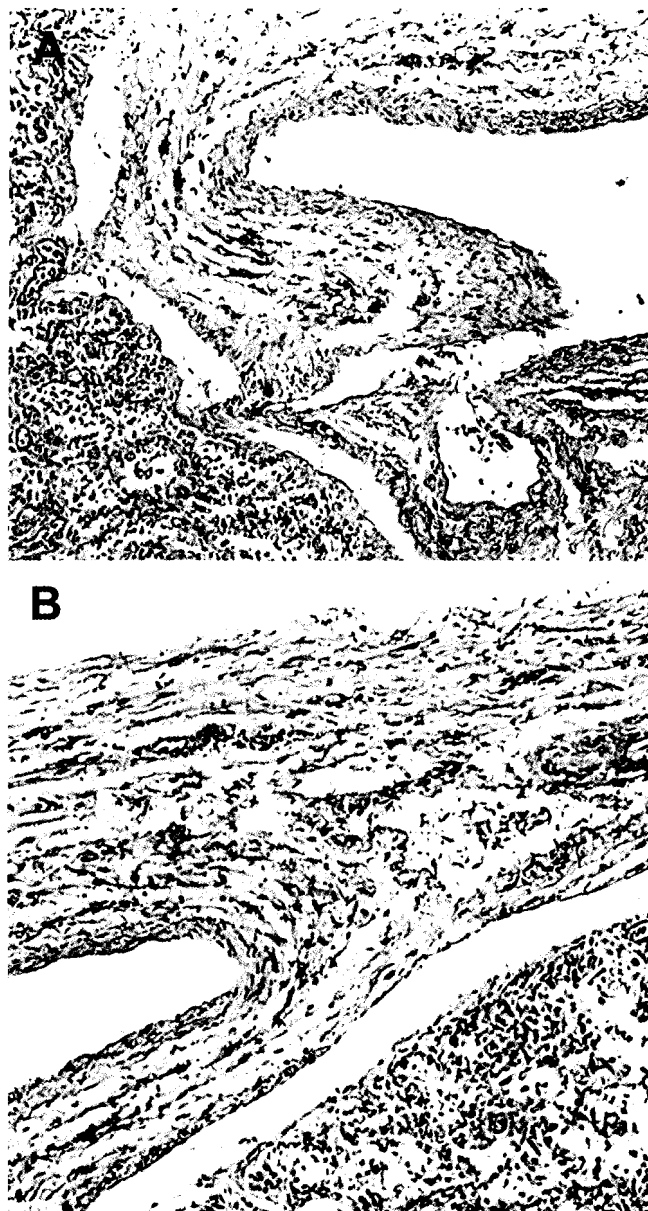


Fig. 5. Histology of a lung specimen from the post-mortem examination of case 3. Panel A (magnification 20x) and panel B (magnification 25x); immunoperoxidase CD34–Q Bend 10; counterstain with hematoxylin. Dilated lymphatic spaces are seen in the sub-pleural connective tissue, along thickened interlobar septa, and around bronchovascular axes. Lymphatic vessels are characterized by a thin wall, devoid of smooth muscle, and slightly dilated lumen, lined by flattened endothelial cells.

nutrition, including the fetus and occasionally the neonate, since elevated triglyceride levels are frequently not detectable in pleural fluid (14). Without enteral feeding, insufficient

chylomicra (the main triglyceride carrier) are produced to raise chyle triglyceride levels. In malnourished patients, a diagnosis of chylothorax is suggested by high lymphocyte

Permission granted for single print for individual use.

Reproduction not permitted without permission of Journal LYMPHOLOGY .

count in the pleural fluid (14). In our cases, the fluid obtained by thoracic drainage was typical of chyle with lactescent appearance after oral feeding and characteristic chemical and cellular composition.

Bilateral pulmonary hyperinflation and increased reticulo-nodular interstitial markings, representing dilated pulmonary lymphatics, are the main radiographic findings in CPL (5). Diffuse thickening of both the peribronchovascular interstitium and the septa surrounding the lobules, as well as patchy ground-glass opacity, are typical features revealed by High-Resolution Computed Tomography. Our cases displayed these radiological findings suggestive of a diagnosis of CPL.

Lung histology in CPL usually shows dilated lymphatic vessels and increased connective tissue in sub-pleural and interstitial locations with thickened interlobular septa in the pulmonary parenchyma. The visceral pleura often displays a cobblestone appearance. The histological findings in case 3 matched these features (*Fig. 5*).

CPL and CC are often described as separate entities. This is most likely due to the small number of existing reports on CPL that include biochemical and cytological analysis of the pleural fluid and the limited number of cases reported of combined CPL and CC, supported by adequate diagnostic studies (5,7).

NIHF has been reported in several congenital disorders, including those with lymphatic maldevelopment. In these cases, the pathogenesis of hydrops fetalis is heterogeneous, but the most likely cause appears to be either a lymphatic block at the entrance site of one or both broncho-mediastinal trunks into the venous system or a blockage of the thoracic duct, causing massive collateral lymph flow through the lungs (15). This pathogenetic sequence suggests that CPL, CC, and NIHF are related entities: the initial (microscopic) dilatation of lymphatic channels gives way to progressive weeping of lymphatics, leading to pleural

effusion, and NIHF may be the final consequence of a superimposed impaired systemic venous return.

Proving this hypothesis is difficult, even by post-mortem examinations. Lung removal during autopsies causes the lymphatics to collapse, thereby preventing the network of intercommunicating channels from being in evidence. Lung cysts disappear when lymph is rapidly drained, as occurs when the lung is removed. Lymphoscintigraphy may provide an important dynamic non-invasive evaluation of lymph flow in the thoracic duct and its tributaries. Evidence of accumulated radioactivity at the mediastinal level and, in particular, signs of backflow from the thoracic duct (*Fig. 4*) are important clues regarding the possible pathogenesis of CC-CPL and perhaps also of NIHF. Retrograde flow from the thoracic duct would lead to accumulation of intestinal lymph within the pleural and pulmonary lymphatic systems. Some authors have suggested that the retrograde pressure might lead to pleural effusion (7 and citations therein) but a definitive demonstration has not been provided.

Evaluation of the lymphatic tracer transport index (*Fig. 4, see legend*) provides a potentially valuable clue, since a quantitative estimate of the degree of obstruction would allow the comparison of patients and could be useful in follow-up. Furthermore, indirect radionuclide lymphoscintigraphy does not necessarily require even minimal sedation, is a safe, reliable, and reproducible method of confirming lymphatic impairment, and is easily performed even during the neonatal period (5,16).

To elucidate the connections among congenital pulmonary lymphangiectasia, congenital chylothorax, non-immune hydrops fetalis and to improve early detection and treatment, further studies should be carried out combining multimodal visualization techniques with and without contrast including lymphangioscintigraphy, computed tomography and magnetic resonance imaging.

REFERENCES

1. Virchow, R: *Gesammelte Abhandlungen zur wissenschaftlichen Medizin*. Frankfurt: Meidinger, Sohn und Co, 1896.
2. Büttiker, V, S Fanconi, R Burger: Chylothorax in children. Guidelines for diagnosis and management. *Chest* 116 (1999), 682-687.
3. van Straaten, HL, LJ Gerards, TG Krediet: Chylothorax in the neonatal period. *Eur. J. Pediatr.* 152 (1993), 2-5.
4. Gilewski, MK, CC Statler, G Kohut, et al: Congenital pulmonary lymphangiectasia and other anomalies in a child: provisionally unique syndrome? *Am. J. Med. Genet.* 66 (1996); 438-440.
5. Chung, CJ, LA Fordham, P Barker, et al: Children with congenital pulmonary lymphangiectasia: after infancy. *Am. J. Roentgenol.* 173 (1999); 1583-1588.
6. Straats, BA, RD Ellefson, LL Budahn, et al: The lipoprotein profile of chylous and nonchylous pleural effusions. *Mayo Clin. Proc.* 11 (1980), 700-704.
7. Moerman, P, K Van den Berghe, H Devlieger, et al: Congenital pulmonary lymphangiectasis with chylothorax. A heterogeneous lymphatic vessel abnormality. *Am. J. Med. Genet.* 47 (1993), 54-58.
8. Njolstad, PR, H Reigstad, J Westby, et al: Familial non-immune hydrops fetalis and congenital pulmonary lymphangiectasia. *Eur. J. Pediatr.* 157 (1998), 498-501.
9. Van Balkom, ID, M Alders, J Allanson, et al: Lymphedema-lymphangiectasia-mental retardation (Hennekam) syndrome: A review. *Am. J. Med. Genet.* 112 (2002), 412-421.
10. Noonan, JA, LR Walters, JT Reeves: Congenital pulmonary lymphangiectasis. *Radiology* 100 (1971), 533-539.
11. Alvarez, JRF, KD Kalache, EL Grauel: Management of spontaneous congenital chylothorax: oral medium-chain triglycerides versus total parental nutrition. *Am. J. Perinat.* 16 (1999), 415-420.
12. Weber, AM, EH Philipson: Fetal pleural effusion: A review and meta-analysis for prognostic indicators. *Obstet. Gynecol.* 79 (1992), 281-286.
13. Hesselting, PB, H Hoffman: Chylothorax: A review of the literature and report of 3 cases. *S. Afr. Med. J.* 60 (1981), 675-678.
14. de Beer, HGJ, MJT Mol, JP Janssen: Chylothorax. *Neth. J. Med.* 56 (2000), 25-31.
15. Jacquemont, S, S Barbarot, M Boceno, et al: Familial congenital pulmonary lymphangiectasia, non-immune hydrops fetalis, facial and lower limb lymphedema: confirmation of Njolstad's report. *Am. J. Med. Genet.* 93 (2000), 264-268.
16. Bellini, C, C Arioni, M Mazzella, et al: Serra: Lymphoscintigraphic evaluation of congenital lymphedema of the newborn. *Clin. Nucl. Med.* 27 (2002), 383-384.

Carlo Bellini, MD, PhD
Dipartimento di Pediatria
Università di Genova
Istituto G. Gaslini,
Largo G. Gaslini, 5
16147 Genova, Italy
Tel: +39 10 5636605
Fax: +39 10 3770675
Email: carlobellini@ospedale-gaslini.ge.it